Localized States at Zigzag Edges of Bilayer Graphene

Eduardo V. Castro,[1] N. M. R. Peres,[2] J. M. B. Lopes dos Santos,[1] A. H. Castro Neto,[3] and F. Guinea[4]

[1]*CFP and Departamento de Física, Faculdade de Ciências Universidade do Porto, P-4169-007 Porto, Portugal*
[2]*Center of Physics and Departamento de Física, Universidade do Minho, P-4710-057 Braga, Portugal*
[3]*Department of Physics, Boston University, 590 Commonwealth Avenue, Boston, Massachusetts 02215, USA*
[4]*Instituto de Ciencia de Materiales de Madrid, CSIC, Cantoblanco, E-28049 Madrid, Spain*

(Received 27 July 2007; published 15 January 2008)

We report the existence of zero-energy surface states localized at zigzag edges of bilayer graphene. Working within the tight-binding approximation we derive the analytic solution for the wave functions of these peculiar surface states. It is shown that zero-energy edge states in bilayer graphene can be divided into two families: (i) states living only on a single plane, equivalent to surface states in monolayer graphene and (ii) states with a finite amplitude over the two layers, with an enhanced penetration into the bulk. The bulk and surface (edge) electronic structure of bilayer graphene nanoribbons is also studied, both in the absence and in the presence of a bias voltage between planes.

DOI: 10.1103/PhysRevLett.100.026802 PACS numbers: 73.20.At, 73.21.Ac, 73.22.−f, 73.63.−b

Introduction.—The quest for new materials and material properties has recently led to graphene, the missing two-dimensional (2D) allotrope of carbon [1]. Stability and ballistic transport on the submicrometre scale, even at room temperature, make graphene based electronics a promising possibility [2]. Indeed, with Si-based technology approaching its limits, a truly 2D material with unconventional electronic properties is regarded with great expectations.

Graphene is a zero-gap semiconductor, and this prevents standard logic applications where the presence of a finite gap is paramount. Band gaps can still be engineered by confining graphene electrons in narrow ribbons [3,4]. However, the lateral confinement brings about the presence of edges, which in graphene can have profound consequences on electronics. This is essentially due to the rather different behavior of the two possible (perfect) terminations in graphene: *zigzag* and *armchair*. While zigzag edges support localized states, armchair edges do not [5–7]. These edge states occur at zero energy, the same as the Fermi level of undoped graphene, meaning that low energy properties may be substantially altered by their presence. The self-doping phenomenon [8] and the edge magnetization with consequent gap opening [9] are among edge states driven effects.

Bilayer graphene, as its single layer counterpart, is also a zero-gap semiconductor [10], but only in the absence of an external electric field: the electronic gap can be tuned externally [11]. Nevertheless, the question regarding the presence of edge states in bilayer graphene is pertinent. First, zigzag edges are among the possible terminations in bilayer graphene, and second, the presence of edges is unavoidable in tiny devices.

In the present Letter we show that zero-energy edge states do exist at zigzag edges of bilayer graphene. An analytic solution for the wave function is given assuming a semi-infinite system and a first nearest-neighbor tight-binding model. The analytic solution we have found defines two types of edge states: monolayer edge states, with finite amplitude on a single plane and bilayer edge states, with finite amplitude on both planes, and with an enhanced penetration into the bulk. A schematic representation of the two families of edge states at $ka/2\pi = 0.35$ can be seen in Fig. 1. We also show that bilayer graphene nanoribbons with zigzag edges have four flat bands occurring at zero energy, a consequence of the two families of edge states localized on each edge. In the case of a biased ribbon, where the two planes are at different electrostatic potentials and a band gap develops for the bulk electronic structure, the spectrum still shows two flat bands while the other two give rise to level crossing inside the gap.

Surface states in semi-infinite bilayer graphene.—The study of edge states in *AB*-stacked bilayer graphene given here is based on the ribbon geometry with zigzag edges shown in Fig. 2. We use labels 1 and 2 for the top and the bottom layers, respectively, and labels Ai and Bi for each of the two sublattices in layer i. Each four-atom unit cell has integer indices m and n such that $m\mathbf{a}_1 + n\mathbf{a}_2$ is its position vector, where $\mathbf{a}_1 = a(1, 0)$ and $\mathbf{a}_2 = a(1, -\sqrt{3})/2$ are the basis vectors and $a \approx 2.46$ Å is the lattice constant. The simplest model describing noninteracting electrons in *AB*-stacked bilayer is the first nearest-neighbor tight-binding model given by

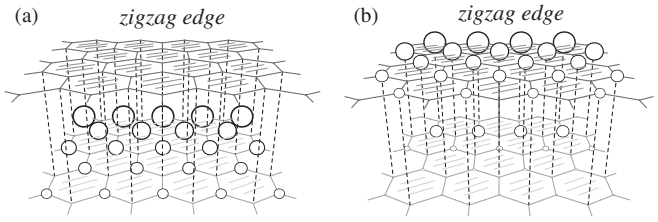

FIG. 1. Charge density for the two families of edge states in bilayer graphene: (a) *monolayer* [Eq. (11)]; (b) *bilayer* [Eq. (12)].

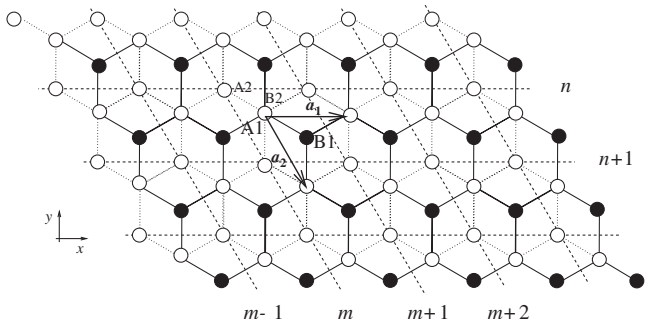

FIG. 2. Bilayer graphene ribbon with zigzag edges.

$$H = -t\sum_{i=1}^{2}\sum_{m,n} a^{\dagger}_{i;m,n}(b_{i;m,n} + b_{i;m-1,n} + b_{i;m,n-1}) - t_{\perp}\sum_{m,n} a^{\dagger}_{1;m,n}b_{2;m,n} + \text{H.c.}, \quad (1)$$

where $a_{i;m,n}$ ($b_{i;m,n}$) is the annihilation operator at position (m, n) in sublattice Ai (Bi), $i = 1, 2$. The first term in Eq. (1) describes in-plane hopping while the second term parametrizes the interlayer coupling ($t_{\perp}/t \ll 1$). Without loss of generality we assume that the ribbon has N unit cells in the y direction with $n \in \{0, \ldots, N-1\}$, and we use periodic boundary conditions along the x direction. This enables the diagonalization of Hamiltonian (1) with respect to the m index just by Fourier transforming along the x direction, leading to $H = \sum_k H_k$, with

$$H_k = -t\sum_{i=1}^{2}\sum_{n} a^{\dagger}_{i;k,n}[(1 + e^{ika})b_{i;k,n} + b_{i;k,n-1}] - t_{\perp}\sum_{n} a^{\dagger}_{1;k,n}b_{2;k,n} + \text{H.c.}. \quad (2)$$

In order to search for zero-energy edge states we solve the Schrödinger equation, $H_k|\psi_k\rangle = E_k|\psi_k\rangle$, for $E_k = 0$. Hamiltonian H_k in Eq. (2) defines a 1D problem in the y direction, and we can write any eigenstate as a linear combination of the site amplitudes along the ribbon's cross section,

$$|\psi_k\rangle = \sum_{n}\sum_{i=1}^{2}[\alpha_i(k, n)|a_i, k, n\rangle + \beta_i(k, n)|b_i, k, n\rangle], \quad (3)$$

where the four terms per n refer to the four atoms per unit cell, to which we associate the one-particle states $|c_i, k, n\rangle = c^{\dagger}_{i;k,n}|0\rangle$, with $c_i = a_i, b_i$, and $i = 1, 2$. In addition, we require the boundary conditions $\alpha_1(k, N) = \alpha_2(k, N) = \beta_1(k, -1) = \beta_2(k, -1) = 0$, accounting for the finite width of the ribbon. It can be straightforwardly shown that if Eq. (3) is a zero-energy solution of the Schrödinger equation, the coefficients satisfy the following matrix equations:

$$\begin{bmatrix}\alpha_1(k,n+1)\\ \alpha_2(k,n+1)\end{bmatrix} = e^{-i(ka/2)}\begin{bmatrix} D_k & 0\\ -\frac{t_{\perp}}{t}e^{i(ka/2)} & D_k\end{bmatrix}\begin{bmatrix}\alpha_1(k,n)\\ \alpha_2(k,n)\end{bmatrix}, \quad (4)$$

$$\begin{bmatrix}\beta_2(k,n-1)\\ \beta_1(k,n-1)\end{bmatrix} = e^{i(ka/2)}\begin{bmatrix} D_k & 0\\ -\frac{t_{\perp}}{t}e^{-i(ka/2)} & D_k\end{bmatrix}\begin{bmatrix}\beta_2(k,n)\\ \beta_1(k,n)\end{bmatrix}, \quad (5)$$

where $D_k = -2\cos(ka/2)$. As the 2×2 matrix in Eqs. (4) and (5) has the following property for any complex p_k,

$$\begin{bmatrix} D_k & 0\\ p_k & D_k\end{bmatrix}^n = \begin{bmatrix} D_k^n & 0\\ nD_k^{n-1}p_k & D_k^n\end{bmatrix}, \quad (6)$$

we conclude by induction that the general solution of Eqs. (4) and (5) has the form:

$$\begin{bmatrix}\alpha_1(k,n)\\ \alpha_2(k,n)\end{bmatrix} = e^{-i(ka/2)n}\mathbf{T}_n\begin{bmatrix}\alpha_1(k,0)\\ \alpha_2(k,0)\end{bmatrix}, \quad (7)$$

$$\begin{bmatrix}\beta_2(k,N-n-1)\\ \beta_1(k,N-n-1)\end{bmatrix} = e^{i(ka/2)n}\mathbf{T}_n^{*}\begin{bmatrix}\beta_2(k,N-1)\\ \beta_1(k,N-1)\end{bmatrix}, \quad (8)$$

for $n \geq 1$, where the matrix $\mathbf{T}_n$ is given by,

$$\mathbf{T}_n = \begin{bmatrix} D_k^n & 0\\ -nD_k^{n-1}\frac{t_{\perp}}{t}e^{i(ka/2)} & D_k^n\end{bmatrix}, \quad (9)$$

and $\mathbf{T}_n^{*}$ is the matrix whose elements are the complex conjugate of $\mathbf{T}_n$. One also requires the convergence condition $|-2\cos(ka/2)| < 1$, which guarantees that the boundary conditions are satisfied for semi-infinite systems. It is easy to see that the semi-infinite bilayer sheet has edge states for k in the region $2\pi/3 < ka < 4\pi/3$, as in the graphene sheet. The next question concerns the number of edge states. As any initialization vector is a linear combination of only two linearly independent vectors there are only two states per edge (per k). Moreover, in the semi-infinite system only half survive, as Eqs. (7) and (8) are edge states solutions on different sides of the ribbon. Taking the limit $N \to \infty$, and choosing the simplest linear independent initialization vectors $[\alpha_1(k, 0), 0]$ and $[0, \alpha_2(k, 0)]$, the two possible edge states are

$$\alpha_1(k, n) = \alpha_1(k, 0)D_k^n e^{-i(ka/2)n}, \qquad \alpha_2(k, n) = -\alpha_1(k, 0)nD_k^{n-1}\frac{t_{\perp}}{t}e^{-i(ka/2)(n-1)}, \quad (10)$$

and

$$\alpha_1(k, n) = 0, \qquad \alpha_2(k, n) = \alpha_2(k, 0)D_k^n e^{-i(ka/2)n}. \quad (11)$$

It is clear that the edge states (10) and (11) are not orthogonal, except for $ka = \pi$. It is convenient to orthogonalize (10) with respect to (11) so that we finally obtain

$$\alpha_1(k, n) = \alpha_1(k, 0)D_k^n e^{-i(ka/2)n}, \qquad \alpha_2(k, n) = -\alpha_1(k, 0)D_k^{n-1}\frac{t_{\perp}}{t}e^{-i(ka/2)(n-1)}\left(n - \frac{D_k^2}{1 - D_k^2}\right), \quad (12)$$

which, together with Eq. (11), represent all possible orthonormalized zero-energy edge states for bilayer graphene.

The normalization constants in Eqs. (11) and (12) are given by $|\alpha_1(k,0)|^2 = (1-D_k^2)^3/[(1-D_k^2)^2 + t_\perp^2/t^2]$ and $|\alpha_2(k,0)|^2 = 1 - D_k^2$. An example of the charge density associated with Eq. (12) is shown in Fig. 3 for $t_\perp/t = 0.2$, where the $|\alpha_1(k,n)|^2$ dependence can also be seen as the solution given by Eq. (11) for $|\alpha_2(k,n)|^2$, apart from a normalization factor.

The solution given by Eq. (11) is exactly the same as that found for a single graphene layer [5,6], where the only sites with nonzero amplitude belong to the A sublattice of layer 2, the one disconnected from the other layer. Solution (12), on the other hand, is an edge state that can only be found in bilayer graphene. The sites of nonvanishing amplitude occur at sublattice A of layer 2, and at sublattice A of layer 1, which is connected to the other layer through $t_\perp$ (see Fig. 1). Had we increased the semi-infinite sheet from the other side of the ribbon, two similar edge states would have appeared in the opposite edge with nonzero amplitudes at sites of the B sublattices. The same value of λ, the penetration depth, is obtained from Eqs. (11) and (12): $\lambda = -1/\ln|D_k|$. Nevertheless, the solution given by Eq. (12) has a linear dependence in n which enhances its penetration into the bulk. We expect these states to contribute more to self-doping then the usual single layer edge states [8], as the induced Hartree potential which limits the charge transfer between the bulk and the edge will be weaker. The key to self-doping is the presence of both an electron-hole asymmetry and extended defects. Electron-hole asymmetry may be due to in-plane next nearest-neighbor hopping (NNN) t', while edges play the role of extended defects. The finite t' shifts the energy of edge states, leading to charge transfer between clean regions and defects. The energy shift for the single layer is given by $E_k \approx -t'(D_k^2 - 1)$ to first order in t', apart from a global factor of $-3t'$ [12]. This is exactly the energy shift we get (away from the Dirac points) for bilayer graphene with in-plane NNN hopping, if we neglect terms of the order $t't_\perp/t$ and higher.

Nanoribbons of bilayer graphene (unbiased).—So far we studied localized states at the semi-infinite bilayer graphene. Experimentally, however, the relevant situation is a bilayer ribbon. The band structure of a bilayer ribbon with zigzag edges is shown in Fig. 4, obtained by numerically solving Eq. (2). We can see four partly flat bands at $E = 0$ for k in the range $2\pi/3 \le ka \le 4\pi/3$, corresponding to four edge states, two per edge. Strictly speaking, the edge states given by Eqs. (11) and (12) [and the other two resulting from Eq. (8)] are eigenstates of the semi-infinite system only. In the ribbon the overlapping of four edge states leads to a slight dispersion and nondegeneracy. However, as long as the ribbon width is sufficiently large, this effect is only important at $ka \simeq 2\pi/3$ and $ka \simeq 4\pi/3$, where λ is large enough for the overlap to be appreciable [7]. As Eq. (12) has a deeper penetration into the bulk, its degeneracy is lifted first, as can be seen in Fig. 4(b). We may then conclude that edge states do exist in bilayer graphene ribbons. We expect band gaps to open due to magnetic instabilities induced by electron-electron interactions, similarly to graphene single layer [5,9]. Actually, the edge states we have found live only on a single sublattice: A or B depending on the edge they are localized. These kinds of localized states favor a ferromagnetic arrangement along the edge and antiferromagnetic between edges [13], consistent with what is found by first principles for stacked graphitic strips [14]. Also half-metallicity should occur in graphene bilayer nanoribbons as a consequence of edge states, analogously to the single layer [15].

Bilayer edge states in different ribbon edges give rise to different intensities in scanning tunneling microscopy (STM). As an example, we consider the ribbon shown in Fig. 2 and assume that the STM signal is essentially proportional to the local density of states of the upper layer. At the top zigzag edge the STM signal is due to edge states of the *bilayer* type, the only ones with finite amplitude on the upper layer [Eq. (12)]. On the other hand, at the bottom zigzag edge both *bilayer* and *monolayer* families have finite amplitude on the upper layer, and a higher STM intensity is expected therefrom.

Nanoribbons of bilayer graphene (biased).—It has recently been shown that the electronic gap of a graphene bilayer can be effectively controlled externally by applying a gate bias [11]. We now consider the case of biased bilayer nanoribbon with zigzag edges, where the presence of edge states should play a role. The bias gives rise to an electrostatic potential difference, V, between the two layers. This is parametrized by adding to the Hamiltonian in Eq. (1) the term $\frac{V}{2}\sum_{m,n}(n_{1;m,n} - n_{2;m,n})$, with $n_{i;m,n} = a^\dagger_{i;m,n}a_{i;m,n} + b^\dagger_{i;m,n}b_{i;m,n}$. Edge states are strongly affected by the bias. The semi-infinite biased system has only one edge state given by Eq. (11), as the edge state having finite amplitudes at both layers [Eq. (12)] is no longer an eigenstate. In Fig. 5

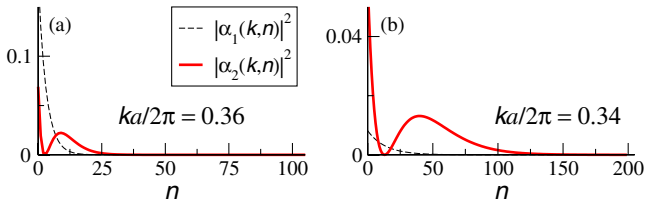

FIG. 3 (color online). Charge density for bilayer edge states at (a) $ka/2\pi = 0.36$ and (b) $ka/2\pi = 0.34$.

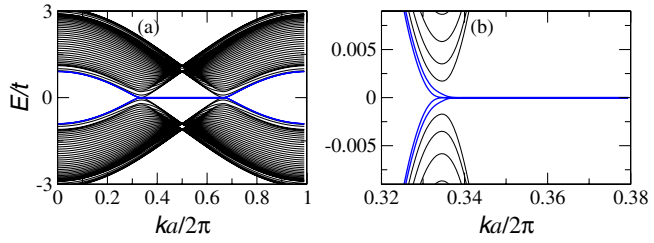

FIG. 4 (color online). (a) Energy spectrum for a bilayer ribbon with zigzag edges: $N = 400$, $t_\perp = 0.2t$. (b) Zoom of (a).

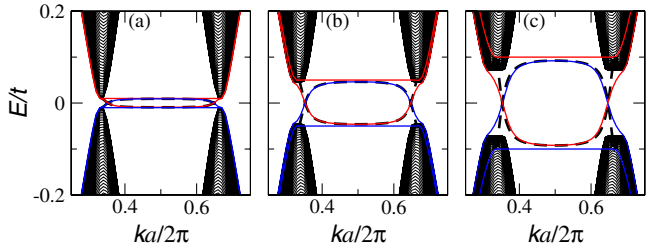

FIG. 5 (color online). Energy spectrum for a bilayer ribbon with zigzag edges, $N = 400$, $t_\perp = 0.2t$: (a) $V = t_\perp/10$, (b) $V = t_\perp/2$, (c) $V = t_\perp$. Dashed lines are from Eq. (15).

we show the band structure of a bilayer ribbon for different values of the bias. Two partially flat bands for k in the range $2\pi/3 \leq ka \leq 4\pi/3$ are clearly seen at $E = \pm V/2$. These are bands of edge states localized at opposite ribbon sides, with finite amplitudes on a single layer [Eq. (11) and its counterpart for the other edge]. Also evident is the presence of two dispersive bands crossing the gap. Both the closeness of these dispersive bands to $E \approx \pm V/2$ for $ka \approx \pi$ and their crossing at $E = 0$ near the Dirac points can be understood using perturbation theory in V/t. As surface states living at opposite edges have an exponentially small overlap, and those belonging to the same edge are orthogonal, we can treat the solution given by Eq. (12) and its counterpart for the other edge separately. Starting with Eq. (12), the first order energy shift induced by the applied bias is $E_k = V/2(\langle n_1^k \rangle - \langle n_2^k \rangle)$, where $\langle n_1^k \rangle$ and $\langle n_2^k \rangle$ give the probability of finding the localized electron in layer 1 and 2, respectively. The value of these quantities is easily obtained from Eq. (12) through a real space summation,

$$\langle n_1^k \rangle = \frac{(1 - D_k^2)^2}{(1 - D_k^2)^2 + t_\perp^2/t^2}, \tag{13}$$

$$\langle n_2^k \rangle = \frac{t_\perp^2/t^2}{(1 - D_k^2)^2 + t_\perp^2/t^2}. \tag{14}$$

The band dispersion is thus given by

$$E_k^\pm = \pm \frac{V}{2} \frac{(1 - D_k^2)^2 - t_\perp^2/t^2}{(1 - D_k^2)^2 + t_\perp^2/t^2}, \tag{15}$$

where the minus sign stands for the band of states localized at the opposite edge. The result of Eq. (15) is shown in Fig. 5 as a dashed line which is hardly distinguishable from the numerical result. Note that for $ka \approx \pi$ we have $D_k \to 0$, so that $E_k^\pm \approx \pm V/2$. This means that for $ka \approx \pi$ the edge state given by Eq. (12) is essentially localized at layer 1, which is clearly seen from Eqs. (13) and (14) as long as $t_\perp/t \ll 1$. For $1 - D_k^2 = t_\perp/t$ the energy shift [Eq. (15)] is zero, which leads to band crossing. For $t_\perp \ll t$ we can expand around the Dirac points, $k_0^\pm a = 2\pi/3, 4\pi/3$. If $k = k_0 + \delta k$, the crossing takes place for $\delta k^\pm a = \pm t_\perp/(t\sqrt{3})$. Note that δk is V independent, and its value compares fairly well with the numerical results shown in Fig. 5. Indeed, the approximate result given by Eq. (15) only fails at the Dirac points, where the edge states localization length diverges and their overlap has to be considered. Increasing the bias makes first order perturbation theory to break down. We have found numerically that the gap opens for $V \gtrsim t$. For $V \lesssim t$ the dispersive states appearing inside the gap may contribute to the finite spectral weight recently observed using angle resolved photoelectron spectroscopy [16].

Conclusions.—We have shown that zero-energy edge states do exist at zigzag edges of bilayer graphene. We have derived an analytic solution for the wave function assuming a semi-infinite system and a first nearest-neighbor tight-binding model. This analytic solution defines two types of edge states: monolayer edge states, with finite amplitude over a single plane, and bilayer edge states, with finite amplitude over the two planes, and with an enhanced penetration into the bulk. Edge states are present even in bilayer graphene nanoribbons, where edge magnetization as well as half-metallicity are expected to show up in analogy with single layer graphene. We have also shown the robustness of bilayer graphene edge states to the presence of an electrostatic potential difference between planes.

E. V. C., N. M. R. P., and J. M. B. L. S. acknowledge financial support from POCI 2010 via Project No. PTDC/FIS/64404/2006 and FCT through Grant No. SFRH/BD/13182/2003. A. H. C. N. was supported through NSF Grant No. DMR-0343790.

[1] K. Novoselov *et al.*, Science **306**, 666 (2004).
[2] A. K. Geim and K. Novoselov, Nat. Mater. **6**, 183 (2007).
[3] Z. Chen *et al.*, arXiv:cond-mat/0701599.
[4] M. Y. Han *et al.*, Phys. Rev. Lett. **98**, 206805 (2007).
[5] M. Fujita *et al.*, J. Phys. Soc. Jpn. **65**, 1920 (1996).
[6] K. Nakada *et al.*, Phys. Rev. B **54**, 17 954 (1996).
[7] K. Wakabayashi *et al.*, Phys. Rev. B **59**, 8271 (1999).
[8] N. M. R. Peres, F. Guinea, and A. H. Castro Neto, Phys. Rev. B **73**, 125411 (2006).
[9] Y.-W. Son, M. L. Cohen, and S. G. Louie, Phys. Rev. Lett. **97**, 216803 (2006).
[10] E. McCann and V. I. Fal'ko, Phys. Rev. Lett. **96**, 086805 (2006).
[11] E. V. Castro *et al.*, Phys. Rev. Lett. **99**, 216802 (2007).
[12] K. Sasaki, S. Murakami, and R. Saito, Appl. Phys. Lett. **88**, 113110 (2006).
[13] E. V. Castro *et al.* (to be published).
[14] H. Lee *et al.*, Phys. Rev. B **72**, 174431 (2005).
[15] Y.-W. Son, M. L. Cohen, and S. G. Louie, Nature (London) **444**, 347 (2006).
[16] T. Ohta *et al.*, Science **313**, 951 (2006).